

Genome-wide remodeling of the epigenetic landscape during myogenic differentiation

Patrik Asp^{a,1,2}, Roy Blum^{a,1}, Vasupradha Vethantham^a, Fabio Parisi^{b,c}, Mariann Micsinai^{b,c}, Jemmie Cheng^a, Christopher Bowman^a, Yuval Kluger^{b,c}, and Brian David Dynlacht^{a,3}

^aDepartment of Pathology and Cancer Institute, New York University School of Medicine, 522 First Avenue, Smilow Research Building 1104, New York, NY 10016; ^bNew York University Center for Health Informatics and Bioinformatics, 550 First Ave, New York, NY 10016; and ^cDepartment of Pathology and Yale Cancer Center, Yale University School of Medicine, 333 Cedar Street, New Haven, CT 06520

Edited* by Robert Tjian, Howard Hughes Medical Institute, Chevy Chase, MD, and approved April 4, 2011 (received for review February 9, 2011)

We have examined changes in the chromatin landscape during muscle differentiation by mapping the genome-wide location of ten key histone marks and transcription factors in mouse myoblasts and terminally differentiated myotubes, providing an exceptionally rich dataset that has enabled discovery of key epigenetic changes underlying myogenesis. Using this compendium, we focused on a well-known repressive mark, histone H3 lysine 27 trimethylation, and identified novel regulatory elements flanking the myogenin gene that function as a key differentiation-dependent switch during myogenesis. Next, we examined the role of Polycomb-mediated H3K27 methylation in gene repression by systematically ablating components of both PRC1 and PRC2 complexes. Surprisingly, we found mechanistic differences between transient and permanent repression of muscle differentiation and lineage commitment genes and observed that the loss of PRC1 and PRC2 components produced opposing differentiation defects. These phenotypes illustrate striking differences as compared to embryonic stem cell differentiation and suggest that PRC1 and PRC2 do not operate sequentially in muscle cells. Our studies of PRC1 occupancy also suggested a “fail-safe” mechanism, whereby PRC1/Bmi1 concentrates at genes specifying nonmuscle lineages, helping to retain H3K27me3 in the face of declining Ezh2-mediated methyltransferase activity in differentiated cells.

chip-Seq | chromatin modifications | muscle development | transcriptional regulation

Regulation of the transcriptome through dynamic changes in chromatin plays an important role in lineage commitment and differentiation. Multiple histone modifications control gene expression through recruitment of factors that alter compaction of the chromatin fiber. Transient and long-term gene silencing is enforced through trimethylation of histone H3 on lysines 9 and 27 (hereafter H3K9me3 and H3K27me3) as well as H4K20, whereas gene activation is regulated by methylation of H3K4 and acetylation of the amino-terminal tails of H3 and H4 (reviewed in refs. 1 and 2). Chromatin modifications are often asymmetrically deposited with respect to the transcription start sites (TSS) of genes. Whereas H3K27me3 is found at promoters, throughout gene bodies, and in intergenic regions, histone tail acetylation and H3K4me3 are predominantly found at promoters and the 5' ends of genes. On the other hand, H3K36 trimethylation marks gene bodies, signifying the passage of RNA polymerase II (PolII) on actively transcribed genes. Promoter acetylation and H3K4 trimethylation are often coordinated, whereas H3K27 and H3K4 trimethylation are largely anticorrelated, except within bivalent regions poised to adopt either active or repressed states at the appropriate developmental stage (3).

Previous studies have shown that the pluripotent state of embryonic stem (ES) cells is in part governed by bivalent nucleosomes, characterized by simultaneous H3K4 and H3K27 trimethylation of nucleosomes in lineage commitment genes (3, 4). During ES cell differentiation, bivalent domains are resolved into regions marked uniquely by H3K4me3 or H3K27me3, resulting in

gene activation or repression, respectively, in accordance with the lineage specified by the marked gene. This mechanism has been shown to be critical for commitment to neuronal and other fates (4). However, despite our understanding of the role of these modifications as “on/off” switches, the epigenetic landscape is considerably more nuanced as a result of the large number of possible permutations specified by modifications of all four histones that dictate both dynamic and irreversible changes in chromatin. Furthermore, although the links between recruitment of Polycomb (PcG) complexes, H3K27 trimethylation, and gene repression have been extensively explored, many questions remain regarding the requirements for PRC1 and PRC2 complexes in gene silencing and their mechanisms of recruitment. For example, because many studies have been conducted in ES cells, one important question concerns the degree to which mechanisms observed in pluripotent cells, distinguished by the prevalence of bivalent promoters, are conserved in committed cells.

Myogenic lineage commitment and execution of the terminal differentiation program depend on the activity of the muscle regulatory factors (MRFs) MyoD1, Myf5, Myf6/MRF4, and myogenin. These transcription factors collaborate with sequence-specific factors, such as MEF2c, cofactors, and histone modifying enzymes to generate transcriptional regulatory networks that promote skeletal muscle differentiation (5). MyoD1 binding coincides with histone acetylation and gene activation (6), whereas H3K27 methylation has been shown to play critical roles in selective repression of muscle-specific genes in growing cells (7–9). Whereas global changes in the epigenetic landscape have been primarily studied during ES cell differentiation, myogenic differentiation has not been comprehensively studied on a genome-wide scale, and the interplay between factors and histone modifications has been studied only on a handful of genes. Using chromatin immunoprecipitation coupled to massively parallel sequencing (ChIP-seq), we have examined the locations of 10 histone modifications and factors in undifferentiated C2C12 myoblasts and fully differentiated myotubes. By merging our ChIP-seq data with expression profiling data, we have assembled and analyzed a rich dataset that has allowed us to begin under-

Author contributions: P.A., R.B., V.V., Y.K., and B.D. designed research; P.A., R.B., V.V., J.C., and C.B. performed research; P.A., R.B., F.P., and M.M. contributed new reagents/analytic tools; P.A., R.B., V.V., F.P., M.M., and B.D. analyzed data; and P.A., R.B., V.V., and B.D. wrote the paper.

The authors declare no conflict of interest.

*This Direct Submission article had a prearranged editor.

Freely available online through the PNAS open access option.

Data deposition: The data reported in this paper have been deposited in the Gene Expression Omnibus (GEO) database, www.ncbi.nlm.nih.gov/geo (accession no. GSE25308).

¹P.A. and R.B. contributed equally to this work.

²Present address: Liver Transplant Program, Montefiore Medical Center, Albert Einstein College of Medicine, 111 East 210 Street, Bronx, NY 10467.

³To whom correspondence should be addressed. E-mail: brian.dynlacht@med.nyu.edu.

See Author Summary on page 8925.

This article contains supporting information online at www.pnas.org/lookup/suppl/doi:10.1073/pnas.1102223108/-DCSupplemental.

standing chromatin modifications underlying differentiation. We have focused on two critical aspects of myogenic differentiation: activation of differentiation-specific gene networks and epigenetic silencing of lineage commitment genes. Whereas confirming several previous observations, our studies (*i*) indicate significant differences between ES cell and skeletal muscle differentiation; (*ii*) highlight a number of unanticipated dynamic changes in histone modifications during muscle differentiation; (*iii*) reveal distinct roles for Polycomb complexes in muscle differentiation; and (*iv*) provide insight into plasticity associated with cells of mesenchymal origin.

Results

Myogenic Differentiation Is Associated with Global Changes in the Epigenetic Landscape. We investigated the epigenetic landscape associated with myogenic differentiation using C2C12 cells, myogenic precursors of mesenchymal origin. We used C2C12 myoblasts because they represent the most widely used and well-established *in vitro* model for mammalian muscle differentiation. In the presence of growth factors, these myoblasts proliferate, but upon shifting to low mitogen conditions, cells efficiently differentiate to multinucleated myotubes. Although these cells have recently been shown to bear a *p19ARF* mutation (10), previous work substantiates the notion that C2C12 cells represent an outstanding model for muscle differentiation. For example, genome-wide expression profiles in primary and C2C12 myoblasts indicated that their transcriptional programs are highly correlated (5). Moreover, ChIP-seq analyses with MyoD1 indicated extremely strong concordance between this cell line and primary cells (6). Furthermore, mapping genome-wide chromatin modifications linked to differentiation requires highly homogenous populations of cells, and we found that C2C12 cells were considerably less prone to spontaneous differentiation than primary myoblasts, making them a more suitable choice for genome-wide analyses (Fig. S1A). We performed western blotting on chromatin isolated from myoblasts and myotubes to determine the global changes associated with myogenic differentiation (Fig. S1B and C). Whereas the majority of modifications remained unchanged during differentiation, there were several significant exceptions. First, there was a robust, global differentiation-dependent decrease in acetylation of histone H3, and a more detailed analysis confirmed this decrease for H3K9Ac and H3K18Ac (Fig. S1B and C). We also saw a similar striking reduction in H4K12Ac in myotubes. Moreover, we detected histone H3 cleavage upon differentiation, consistent with a previous report showing that the N-terminal tail of this histone is cleaved (at residues 22–23) during ES differentiation (11), and suggesting that this could represent a common feature of differentiation (Fig. S1B). Thus, a global reduction in overall H3 acetylation could be ascribed either to N-terminal cleavage, preferential deacetylation by histone deacetylases in myotubes, or both. In contrast to acetylation, significant global changes in trimethylation of H3K4, H3K36, and H3K27 were not detected during differentiation (Fig. S1B).

Genome-Wide Identification of Chromatin Marks Associated with Myogenic Differentiation. To examine changes in chromatin on a genome-scale, we performed ChIP-seq in growing myoblasts and myotubes, selecting marks and factors associated with promoters and enhancers (H3K4me1, H3K4me2, H3K4me3, H3K9Ac, H4K12Ac, H3K18Ac, PolII) or gene bodies (H3K36me3), as well as marks more widely distributed in euchromatin and heterochromatin (H3K9me3, H3K27me3) with antibodies whose specificity had been verified (Figs. S1D and S24; see also *SI Materials and Methods*). Three to four independent libraries were sequenced for each mark/factor after subjecting libraries to extensive quality controls (*Materials and Methods*). This approach enabled us to reach a similar sequencing depth for all marks or factors that surpassed most genome-wide

ChIP-seq studies of histone modifications published to-date (Fig. S2B and *SI Materials and Methods*).

When we commenced our genome-wide effort, we found that available peak-finding algorithms failed to detect a substantial number of histone modification events in our data. Therefore, we developed and extensively tested a peak-finding algorithm, Qeseq, which enabled us to identify both narrow peaks for factor binding and broader peaks associated with chromatin modifications (*SI Materials and Methods*). First, we validated a select number of peaks by performing ChIP in primary mouse myoblasts and myotubes (Fig. S2C). Next we validated a significant number of sites identified by Qeseq using ChIP-qPCR, and together these analyses confirmed the robust and reliable performance of our algorithm (Fig. S2D). Finally, Qeseq performance was tested and compared to several other peak-finding algorithms in a more comprehensive and unbiased manner by extensive validation of over 300 different loci marked with H3K27me3 and H3K36me3 using ChIP-qPCR. This comparative analysis demonstrated that our algorithm matched or surpassed the performance of previously existing peak-finding programs in its ability to detect enrichment of histone modifications and factors in our ChIP-seq data. Our algorithm allowed us to compute enrichment scores and *p*-values for each event after comparison with controls consisting of MNase-treated or sonicated input chromatin. Importantly, our analysis globally captured well-established epigenetic observations, including widespread modification of *HOX* clusters and relative enrichment of all histone marks with respect to the TSS and gene bodies (Fig. 1 and Figs. S2E and S3).

Expression profiling of C2C12 myoblasts and myotubes (12, 13) allowed us to subdivide our ChIP-seq data into four expression groups comprised of genes that are (*i*) permanently silenced in both conditions (“never expressed”), (*ii*) constitutively expressed at equal levels (“constitutive”), and (*iii* and *iv*) up- or down-regulated in myotubes (Fig. S1D; *SI Materials and Methods*). This approach allowed us to quantitatively associate epigenetic patterns with dynamic changes in expression during myogenic differentiation (Fig. 1 and Fig. S3). We also created analogous profiles based on absolute expression levels and correlated epigenetic patterns with overall expression levels (*SI Materials and Methods* and Fig. S4).

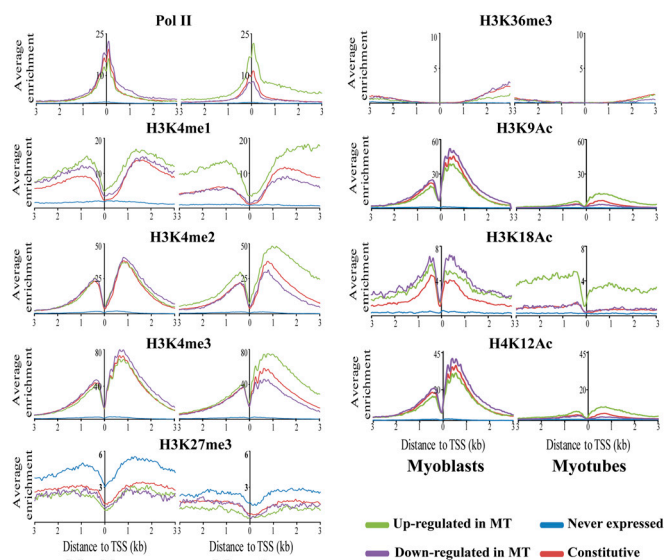


Fig. 1. Dynamic changes in Pol II binding and epigenetic marks associated with differentiation. The average ChIP-seq enrichment per 50 bp bin for the total population of genes in the four dynamic expression groups (*SI Materials and Methods*) were plotted ± 3 kb of the TSS and as a percentage of gene body length (see also Figs. S3 and S4). The y-axis shows the average \log_2 of the enrichment.

Our ChIP-Seq data globally reflected our western blot analyses of total chromatin (Fig. S1B). For each expression group, we saw a near-complete loss of H3K9 and H4K12 acetylation in myotubes (Fig. 1 and Figs. S3 and S4). In contrast, H3K18Ac levels dramatically decreased only on genes that were constitutively expressed or whose expression decreased in myotubes, but levels remained high on genes induced in myotubes. We also observed that, in contrast to H3K9Ac and H4K12Ac, which were restricted to regions surrounding the TSS, H3K18Ac was also present within gene bodies and intergenic regions (Fig. 1 and Figs. S3 and S4).

Genes up-regulated in myotubes showed considerable enrichment for PolIII and active histone marks in cycling myoblasts, suggesting that these genes have already adopted features of active chromatin prior to maximal expression (Fig. 1). Further, these genes had higher levels of PolIII, H3K4me3, H3K4me2, and H3K36me3 in gene bodies in myotubes as compared to genes expressed at similarly high levels in myoblasts (Fig. S3). Taken together, our results show that (i) myoblast chromatin is marked for subsequent robust elevation of gene expression in myotubes and (ii) overall, histone acetylation decreases during myogenic differentiation. Interestingly, MyoD binding has been correlated with regions of elevated H4Ac (6), suggesting that discrete regions may be selectively hyper-acetylated in myotubes through the action of MyoD within a hypo-acetylated landscape.

High-Density Maps (HDM) Identify Marks Associated with Gene Activation and Permanent Repression. We refined our analysis by plotting the ChIP-seq data as nonquantitative HDMs of histone marks and factor binding over regions spanning -3 kb upstream to $+9$ kb downstream of the TSS (Fig. 2 and *SI Materials and Methods*). For the purposes of this study, we focused primarily on genes that were up-regulated in myotubes or permanently silenced in both conditions, as genes in both groups play an important role in muscle development and lineage commitment, respectively (Fig. 2A and B). Remarkably, we found that within a given expression group, genes could be divided into subclusters based on distinct combinations of marks, and these clusters were largely self-contained within specific gene ontology (GO) categories (Fig. S5 and Dataset S1). These divisions did not simply reflect differences in expression levels, because each subcluster exhibited a wide range of gene expression levels, and instead, it suggests that functionally related genes may be specifically demarcated by individualized combinations of marks, irrespective of expression state.

First, we focused on genes up-regulated in myotubes, which could be divided into seven distinct clusters (Fig. 2A and Dataset S1). In myoblasts, where expression of these genes was relatively low, clusters 1 and 2 nevertheless showed strong PolIII binding on many genes near the TSS, suggesting that these genes were marked for activation. Differentiation associated transcriptional up-regulation or activation of these genes led to a clear spreading of PolIII to regions downstream of the TSS, consistent with active transcription. Interestingly, this accumulation of PolIII on genes expressed at low levels in myoblasts was not evident in other clusters (3–7), despite the fact that they were up-regulated to a comparable degree with clusters 1 and 2. Further, virtually no PolIII was detected on genes in clusters 3–4, which were heavily trimethylated on H3K27 in myoblasts, consistent with an inverse connection between this mark and PolIII loading, as suggested previously (14). The densities and levels of H3K4me2/3 around the TSS increased significantly for all clusters during differentiation, in agreement with their enhanced transcriptional activity in myotubes (Figs. 1 and 2 and Fig. S3). In contrast, the distribution of H3K4me1 changed little during myogenesis. Interestingly, clusters 3 and 4 were densely marked in myoblasts by H3K27me3, a modification known to play an essential role in myogenic differentiation (Fig. 2A). Indeed, these clusters were strongly enriched for genes involved in muscle de-

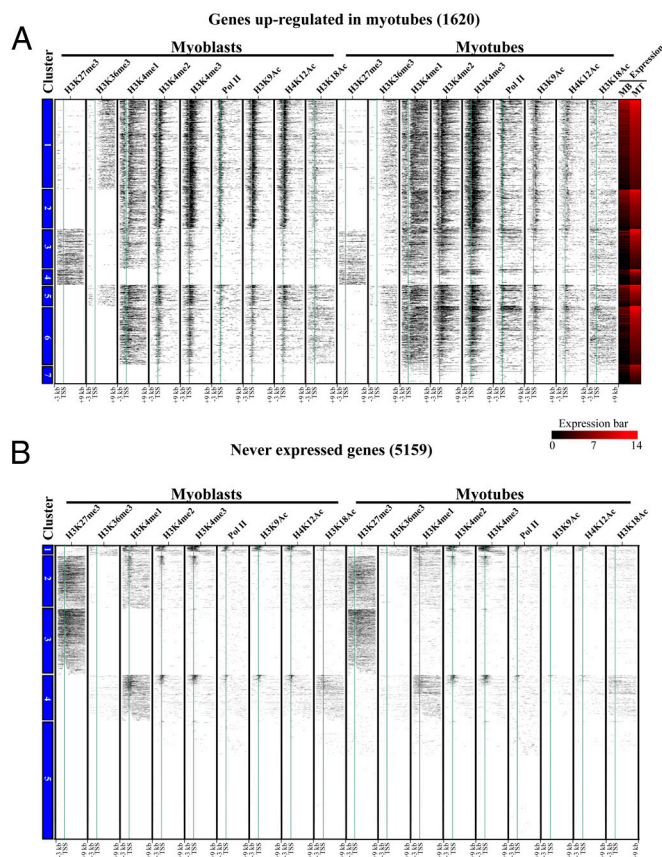


Fig. 2. HDM of Pol II and histone marks in myoblasts and myotubes. Density maps were generated for the region -3 kb to $+9$ kb of the TSS, as described in *SI Materials and Methods*, for (A) genes up-regulated during myogenesis and (B) permanently repressed genes.

velopment (such as *Myog*, *Acta1*, and *Myh3*), and GO analysis identified several subcategories of genes essential for muscle formation (Fig. S5B and Dataset S1). A subset of these genes, including *Myog* (see below), showed a significant reduction in the density of this mark, consistent with previous studies performed on a small number of genes (7, 8). Unexpectedly, other genes in these clusters were transcriptionally up-regulated in myotubes, although they retained H3K27me3 and displayed very low levels of H3K36me3 in both conditions. These results suggest that H3K27 trimethylation alone is not sufficient to suppress gene expression, reminiscent of observations in ES cells (15).

Next, we focused on permanently silenced genes, which segregated into three major clusters and several GO categories (Fig. 2B and Dataset S1). Two clusters were heavily marked with H3K27me3 (clusters 2 and 3) and were distinguished by an overrepresentation of genes involved in cell fate commitment and differentiation pathways distinct from muscle development, with a strong enrichment for genes encoding transcription factors (Fig. 2B, Figs S5A and S6, and Dataset S1). Genes in two *HOX* clusters (*HoxB* and *HoxD*) and those encoding endodermal and ectodermal fate determinants exhibited high-density H3K27me3 modifications (Fig. S2E), as did genes involved in neuronal, brain, and immune system development. In contrast, there was a notable absence of genes involved in myogenesis, osteogenesis, and adipogenesis, all facets of mesoderm development (Figs. 2B, Fig. S5A, and Dataset S1). Interestingly, we found that the few mesoderm-related genes represented in this group are known inhibitors of myogenesis (*Twist*, *Fli1*, *PRDM16*) and are all heavily marked by H3K27me3 (Fig. S6). Extensive H3K27 trimethylation on genes in these clusters could pose a nearly insurmountable

barrier to reactivation in skeletal muscle, thereby preventing differentiation into nonmesodermal lineages.

A second group of permanently silenced genes (clusters 4 and 5) was devoid of all histone modifications that we examined. Strikingly, many members of this group could be sorted into gene families (Fig. 2B and Dataset S1), and many of these gene families were found in clusters on chromosomes, suggesting that gene neighborhoods (or possible chromatin domains) can also be defined by the absence of histone marks. Surprisingly, a smaller group exhibited monomethylation of H3K4 in both states but lacked virtually all other marks. These results suggest that irreversible silencing results largely from one of two states: dominant, widespread coverage with H3K27me3 or a default state in which neither active nor repressive marks (within the limits of this study) are present.

The Role of H3K27me3 in Myogenic Differentiation. H3K27me3 is known to regulate myogenic differentiation through silencing of muscle-specific genes and cell cycle genes in myoblasts and myotubes, respectively (7, 8). In other studies, H3K9me3 was implicated in shutting off cell cycle genes during muscle differentiation (16). However, our ChIP-seq analyses do not support a role for H3K9me3 in repression of cell cycle genes, nor was this mark generally enriched at protein-coding genes (approximately 70% of peaks were not assigned to genes, which encompass coding regions and 3 kb of upstream sequence; Fig. S2B). H3K9me3 peaks were assigned to 109 genes in myoblasts and 276 genes in myotubes (including 25 common genes), but no GO category was significantly enriched as compared to a background set of all mouse genes. H3K9me3 was primarily found within noncoding regions as well as repetitive sequences that could not be uniquely aligned to the mouse genome (Fig. S2B), in line with previous findings (17). We conclude that H3K9 trimethylation does not globally contribute to the differential regulation of gene expression during myogenesis.

In striking contrast, H3K27me3 was widely distributed throughout the genome in both myoblasts and myotubes, encompassing promoters, gene bodies, and intergenic regions (Fig. 3A and B). Approximately 45% of all H3K27me3 marked regions were localized to genes (from -3 kb upstream of the TSS to the transcription termination site) in both conditions, and, as expected, there was a strong anticorrelation with active chromatin marks (Figs. 2A and 3A and B). Despite the widespread nature of this mark, H3K27me3 peaks were often restricted to regions surrounding actively transcribed regions (Fig. 3A and B). The *Myh* cluster, which consists of skeletal muscle myosin heavy chain genes, represents a particularly striking example (Fig. 3B). H3K27me3 disappears over gene bodies (*Myh1*, *Myh3*) or promoters only (*Myh2*, *Myh4*), coincident with induction in myotubes. On the other hand, H3K27me3 further accumulates over *Myh13*, which is not expressed.

We also examined the existence of bivalent promoters in myoblasts and myotubes (here, we restrict this definition to include the presence of H3K27me3 and H3K4me3 on fragments that overlap within nucleosome-sized windows up to 3 kb upstream of the TSS). In ES cells, 22% of genes exhibit bivalent signatures (4). In contrast, only approximately 11% ($n = 436$) of all genes marked by H3K27me3 in myoblasts were bivalent, and only a small portion of those genes were resolved to a monovalent state after differentiation (70 vs. 86 genes were resolved to K27me3 and K4me3, respectively) (Fig. S7A). This bivalent group largely consisted of developmentally relevant genes, in particular, regulators of neurogenesis (Fig. S7B). These results agree with previous studies indicating that resolution of the bivalent state is nearly complete in committed cells (4). With the exception of the small number of bivalent genes that were resolved during differentiation, H3K27me3 was remarkably stable during differen-

tiation, because approximately 90% of all genes bearing H3K27me3 retained this mark during myogenesis (Fig. 2).

C2C12 cells are readily converted to myotubes upon depletion of mitogens, but they are also capable of transdifferentiating into adipocytes and osteoblasts upon exposure to appropriate inducers (18, 19). The absence of GO categories related to osteogenesis or adipogenesis in the group of genes enriched in H3K27me3 indicated that the corresponding genes were not generally marked with this modification. To this end, we investigated chromatin marks on master regulators of osteogenesis and chondrogenesis (*Runx2*, *Sox5*, *Sox6*, and *Sox9*) and adipogenesis (*PPAR γ* , *C/EBP β* , and *C/EBP δ*) and found that these genes bore signatures of gene activation (marked by combinations of enhanced binding of p300 or PolII, H3/H4 acetylation, and H3K4me2/3) and were expressed (Figs. S64 and S84). Further, they were devoid of repressive methylation marks and were not bivalent. Remarkably, these positive signatures were retained on each of these genes in myotubes, and H3K27me3 was not detectable. Certain genes exhibited both active and repressive marks (*C/EBP α*) (Fig. S84). Interestingly, however, several important downstream effectors of these pathways (e.g., *Osterix*, *Alpl*) were solely marked by H3K27me3, suggesting that although key master regulatory genes are expressed, activation of essential downstream effectors awaits additional cues to specify alternative mesodermal fates (Fig. S64).

Identification of Myogenin Regulatory Elements. We asked whether our genome-wide chromatin modification data would enable us to identify regulatory elements relevant to myogenic differentiation, and in the remainder of our study, we focused primarily on the H3K27me3 mark. We examined genes with a prominent role in differentiation, namely, MRF genes, investigating H3K27me3 to determine whether expression of these “master” regulators, and in turn, myogenesis, is controlled through this modification. Interestingly, only one MRF gene, *Myog*, was marked by H3K27me3 (Fig. 3C), whereas all other genes (*Myod1*, *Myf5*, *Myf6/MRF4*) were completely devoid of this modification (Fig. S8B). Our ChIP-seq analysis identified myoblast-specific H3K27me3 enrichment at several genomic regions between 1.5 and 18 kb upstream of the *Myog* TSS, and we verified this enrichment using qPCR (Fig. 3C and F). Several of these peaks were narrow and sharply contrasted with the extended regions of H3K27me3 that encompassed many permanently silenced genes (Fig. 3B and Fig. S2E). We did not observe enrichment for H3K27me3 at the proximal promoter, in agreement with other studies (7), but in contrast with those from another group (9). Further, we found that H3K27 methylation was restricted to myoblasts and that it completely disappeared in myotubes, coinciding with a dramatic elevation in H3K4me3 and gene expression (Fig. 3C).

The binary nature of the H3K27me3 mark prompted us to inspect the *Myog* gene for recruitment of factors and the presence of histone marks indicative of gene activation and repression. We examined our ChIP-seq data, focusing on several regions upstream and downstream of the TSS (Fig. 3C). Apart from H3K4me2/3, we observed H3K4me1 and p300 peaks over several regions in myotubes only. Interestingly, PolII occupied a subset of overlapping regions in myotubes. H3K4me1, p300, and PolII have been associated with transcriptional enhancers (20–22). With the exception of a region downstream of *Myog*, there was no enrichment at these positions for H3K4me3, a well-established indicator of transcription start sites, in either myoblasts or myotubes, suggesting that they are not likely to correspond to previously uncharacterized promoters, and no transcripts that originate from this position have thus far been described.

We further tested the idea that one or more of these regions that were differentially marked by H3K27me3 in myoblasts and H3K4me1, p300, and PolII in myotubes might represent condi-

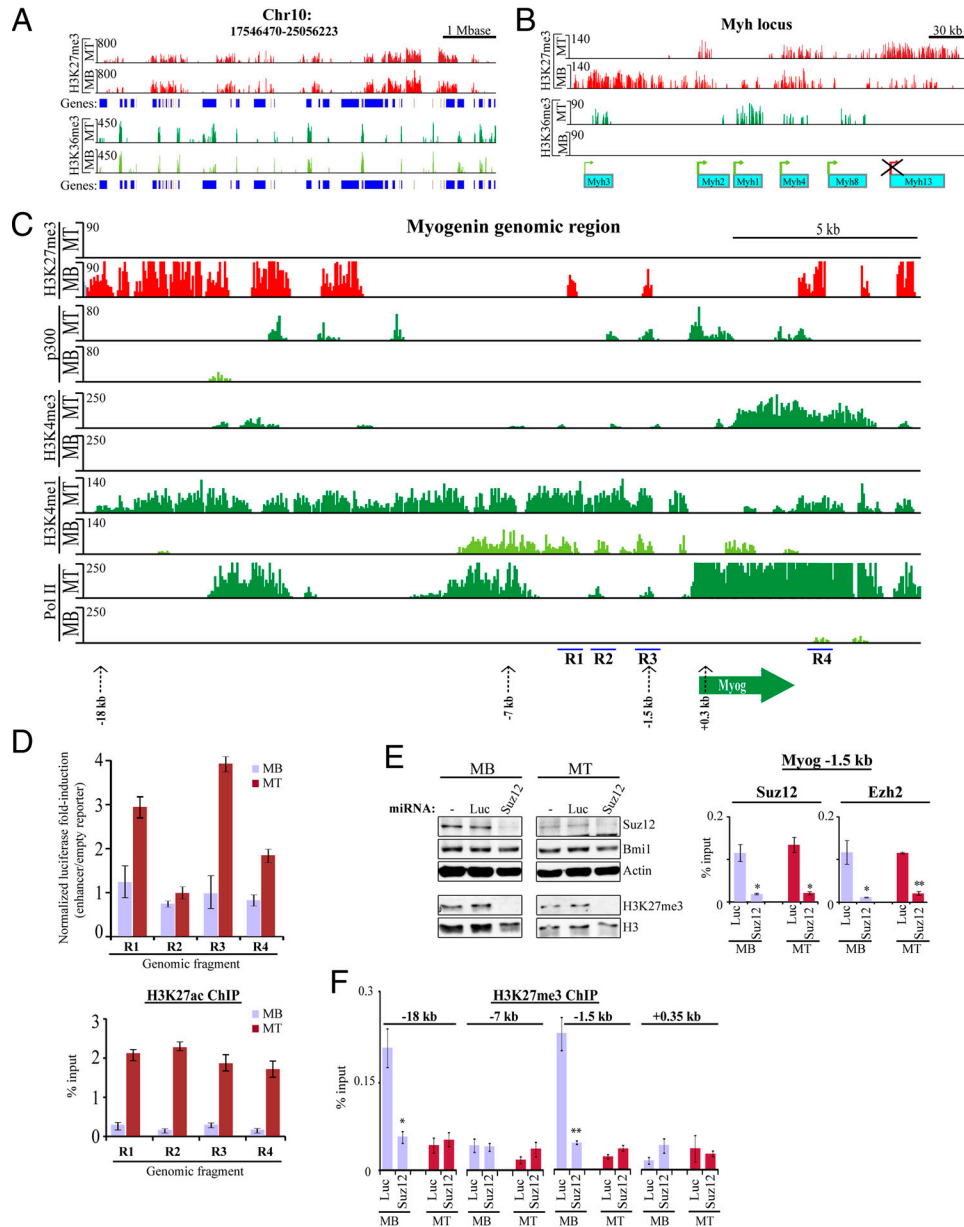


Fig. 3. Characterization H3K27me3 localization and its role in myogenesis (A, B) Patterns of H3K27me3 and its anticorrelation with H3K36me3 across a region of chromosome 10 (Left) and the *Myh* loci (Right). The y-axis shows the \log_2 of the enrichment. (C) ChIP-seq localization of H3K27me3, p300, H3K4me1/3, and Pol II on *Myog*. Blue bars at the bottom indicate fragments tested for enhancer activity. The y-axis shows the \log_2 of the enrichment. (D) Luciferase assay testing the enhancer activity of fragments up- and downstream of *Myog* coding region. (E) Analysis of extracts and chromatin after miRNA-mediated Suz12 depletion in myoblasts and myotubes showing effect on indicated proteins and global H3K27me3 levels by Western blotting (Left) and recruitment to chromatin by ChIP (Right). (F) Quantitative chromatin IP (qChIP) showing the effect of Suz12 depletion on H3K27me3 levels at *Myog* genomic regions shown in panel C.

tion-specific enhancers. We examined one downstream and several upstream regions by inserting each 2 kb downstream of a minimal promoter driving luciferase expression, transfecting C2C12 cells, and inducing differentiation (Fig. 3D). Interestingly, we found that two regions marked by H3K27me3 in myoblasts, located approximately 4 kb (region 1; R1) and approximately 1.5 kb (region 3; R3) upstream of the *Myog* TSS, enhanced expression three- to fourfold, respectively, in myotubes, whereas an intervening region (R2) failed to augment reporter expression (Fig. 3D). In further support of the notion that these regions represent enhancers, each region showed significant, myotube-specific enrichment for H3K27ac, another mark associated with this regulatory element (Fig. 3D). A third segment (R4) downstream of the TSS that was marked by H3K27me3 in myoblasts also showed moderate enhancer activity. Enhancer activity was

not detectable in myoblasts, suggesting differentiation-dependent enhancer activity. Thus, we suggest that *Myog* expression is regulated by a switch in which acetylation replaces methylation on H3K27 in differentiated cells, concomitant with gene expression. Importantly, although each of the regions tested showed one or more enhancer-associated signatures, only a subset of the genomic fragments exhibited enhancer activity, suggesting an as yet unexplored complexity regarding enhancer usage in muscle cells and indicating that the presence of multiple signatures or the absence of a specific mark cannot always predict enhancer function.

Functionally important regulatory elements are often found within evolutionarily conserved regions, and we examined conservation of each genomic fragment (R1-4) within the mouse *Myog* locus. Each enhancer fragment was indeed highly conserved from rodents to humans, in contrast with R2, which was significantly

less conserved (Fig. S8C). Although we have not exhaustively investigated the entire 18 kb region upstream of the *Myog* TSS, which could include additional enhancer elements, our findings strongly suggest the existence of previously undisclosed transcriptional enhancers of the *Myog* gene that are negatively regulated by H3K27me3. These elements were not detected using a candidate approach (7, 9), further illustrating the utility of our genome-wide compendium of histone modifications for discovery of functional regulatory elements.

Next, we searched for transcription factor (TF) binding sites in R1, R2, and R3 using the CLOVER algorithm (23). We found that several position weight matrices corresponding to known TF binding sites were enriched with significant *p*-values within these regions, including Sp1, MyoD1, as well as ZEB1 and several other zinc-finger/Kruppel-like TFs. Although in-depth exploration of these factors must await further studies, enrichment of ZEB1 binding sites is potentially interesting, because it was shown to be a repressor that regulates muscle differentiation by binding to E-boxes and antagonizing MEF2c activity (24).

The Role of Polycomb Complexes. We further investigated the role of H3K27me3 in *Myog* regulation and myogenic differentiation by examining PRC2, the complex required for this modification. The PRC2 complex is comprised of several components, including Suz12, EED, and either Ezh1 or Ezh2, the methyltransferases responsible for H3K27 trimethylation. We focused on the R3 element approximately 1.5 kb upstream of the TSS, because it exhibited substantial enhancer activity, and used ChIP to show that Suz12 and Ezh2 are indeed recruited to this element in myoblasts (Fig. 3E). Interestingly, we note that PRC2 is retained on the R3 element in myotubes, despite the fact that H3K27me3 disappears from this position during differentiation. It has been shown that the *Myog* promoter is demethylated by UTX, an H3K27me3 demethylase in a differentiation-dependent manner (9). The absence of H3K27me3 from R3 in myotubes could therefore result from a competitive situation in which UTX activity exceeds that of PRC2.

Suz12 is required for PRC2 activity, and ablation of Suz12 results in PRC2 destabilization and loss of H3K27me3 in ES cells (15). Therefore, we depleted Suz12 from myoblasts with two distinct synthetic microRNAs (miRNAs) (which yielded identical results) and analyzed the impact on H3K27 methylation, gene expression, and myogenic differentiation. Suz12 depletion led to dramatic reductions in Suz12 and H3K27me3 levels, as expected, and qChIP analysis confirmed depletion of Suz12 and H3K27me3 over several *Myog* upstream regions, including the R3 enhancer (Fig. 3E and F).

First, we analyzed the impact of Suz12 ablation on *Myog* expression, which is detectable as cells become quiescent prior to expression of differentiation markers. Interestingly, we found that *Myog* expression was not induced in Suz12-depleted myoblasts (Fig. 4A). However, *Myog* expression was prematurely and substantially elevated in differentiating Suz12-depleted cells exiting the cell cycle ($T = 0$ h) as compared to controls, suggesting that loss of H3K27me3 acts in concert with other cues, such as growth arrest, to regulate *Myog* expression. We asked whether aberrant *Myog* up-regulation could influence expression of its target genes. Previous ChIP-on-chip analyses identified a group of myogenin targets (5, 6), and we examined two *Myog* targets (*MEF2c* and *Acta1*) and another gene essential for differentiation (*Myh4*). We found that each of these genes was significantly up-regulated in response to Suz12 depletion and elevated expression of myogenin, indicating that premature loss of *Myog* repression likely induces expression of target genes (Fig. 4A).

These findings prompted us to investigate how Suz12 loss could impact differentiation. We ablated Suz12 in myoblasts, induced cells to differentiate, and examined expression of a terminal differentiation marker, myosin heavy chain (MHC), at

various intervals before and after induction of differentiation. Consistent with our gene expression analysis, we found that Suz12 ablation markedly accelerated myogenic differentiation (Fig. 4B). In addition, we observed a 2-fold increase in the number of myotubes (with a concomitant decrease in the population of undifferentiated cells) upon terminal differentiation, suggesting that Suz12 loss increased the number of fusion events (T96h; Fig. 4B). Thus, Suz12 depletion and loss of H3K27me3 accelerated and enhanced the extent of differentiation. Interestingly, these results differ dramatically from those using *Suz12* $-/-$ or EED $-/-$ ES cells, because ablation of either gene impaired differentiation (15, 25) (see Discussion).

To further characterize the role of PcG complexes in transcriptional regulation of *Myog*, we investigated the recruitment of PRC1 to the -1.5 kb (R3) upstream enhancer element. The PRC1 complex, which is recruited to chromatin marked by H3K27me3 and which consists of Bmi1, Ring1A/1B, PC, and PH proteins, enforces silencing through ubiquitylation of H2A and through chromatin compaction (26, 27). Intriguingly, however, we did not detect recruitment of PRC1 in myoblasts, despite the presence of H3K27me3 over the same region (Figs. 3F and 4C). This suggests that repression of *Myog* in myoblasts is mediated by PRC2-dependent deposition of H3K27me3 without detectable PRC1 recruitment.

Together, our experiments suggest that *Myog* is unique among the group of MRFs as a critical target of PRC2 and that H3K27 methylation and demethylation underlie a switching mechanism that controls differentiation. In this setting, the loss of H3K27me3 from *Myog* upstream regulatory sequences could determine the timing of expression of this master regulator and differentiation.

Genes Induced During Differentiation Are Uniquely Susceptible to Suz12 Loss. Given that Polycomb-dependent H3K27 trimethylation plays a pivotal role in the regulation of *Myog* expression and myogenic differentiation, we further explored the role of this repressive machinery on a substantially larger set of genes. Our histone modification maps suggested the existence of two classes of genes marked with H3K27me3: a large group of permanently repressed genes that maintained the mark throughout myogenesis (Fig. 2B, clusters 2 and 3) and a smaller group of genes (including *Myog*) that was up-regulated and lost this mark during differentiation (Fig. 2A, clusters 3 and 4). We analyzed H3K27me3 levels and the recruitment of Polycomb complexes to determine whether additional features might distinguish these two classes of genes. We found that permanently silenced genes exhibited, on average, up to an order of magnitude greater enrichment for H3K27me3 than genes that were expressed under any condition (Fig. 4E). This finding suggested a strong correlation between permanence of gene repression and the levels of this modification.

Next, we examined H3K27me3 levels after Suz12 depletion on both sets of genes. Genes that were induced in myotubes lost H3K27me3 in response to Suz12 depletion, and displayed premature and enhanced expression of target genes, similar to *Myog* (Fig. 4D and E and Fig. S9A). In contrast, genes that were permanently silenced exhibited a differentiation-dependent increase in H3K27me3 levels, but, remarkably, Suz12 depletion did not provoke the loss of H3K27me3 in either myoblasts or myotubes (Fig. 4E and Fig. S9A). Antibody and chromatin titrations ruled out the possibility that antibody concentrations were limiting, thereby preventing our ability to detect changes in H3K27me3 enrichment. Importantly, we could not detect transcripts corresponding to this group of permanently repressed genes before or after Suz12 depletion. These findings suggest that there are two classes of genes marked with H3K27me3: One class shows comparatively low levels of enrichment for H3K27me3, and the existence of this mark depends on recruitment of Suz12. This

We asked whether codepletion of Suz12 and Bmi1 could reverse the differentiation defect associated with Bmi1 or Ring1B loss alone (Fig. 5 *B* and *C*). However, we found that differentiation was significantly compromised in cells lacking both proteins, despite marked reductions in total H3K27me3 (Fig. 5*B*). These findings indicate that PRC1 and PRC2 loss are not equivalent in muscle cells and that loss of PRC1 predominates over PRC2.

Discussion

In this study, we provide a comprehensive genome-wide view of chromatin modifications in cells undergoing skeletal muscle differentiation. Whereas several findings in other systems correlate with our genome-wide studies, other global observations unexpectedly and dramatically differ from what was previously observed in ES cells, substantiating the need to obtain tissue- and cell-type specific profiles for genome-wide modifications. Our ChIP-seq compendium thus provides a rich resource for detailed mechanistic studies and represents a necessary first step toward understanding epigenetic changes that occur during myogenic differentiation.

Distinct Populations of Chromatin Marked by H3K27me3. One major conclusion from our studies is that all segments of chromatin marked with H3K27me3 are not functionally equivalent. Our data support the existence of two classes of genes: one group of genes (class II) is associated with commitment to nonmuscle lineages, is permanently silenced, and exhibits the highest levels of H3K27me3, whereas class I genes are less highly enriched for H3K27me3 and are induced during differentiation. Surprisingly, we found that class II genes exhibited little or no change in recruitment of PRC2, deposition of H3K27me3, or gene expression in response to Suz12 depletion. In contrast, class I genes were sensitive to Suz12 ablation, exhibiting marked reductions in H3K27me3, diminished recruitment of PRC2, and elevated expression. Further, although Bmi1 was highly enriched on class II genes, the protein was largely absent from class I genes that were conditionally repressed in myoblasts. These findings suggest the possibility that the presence of PRC1 stabilizes H3K27me3, making it independent of PRC2 activity. This back-up mechanism would seem to ensure the retention of H3K27me3 on genes that must be silenced in the face of declining levels of Suz12 (Fig. 3*E*) and Ezh2, which essentially disappears in myotubes and in the developing myotome (7). Moreover, because PRC1 is recruited to nucleosomes marked by H3K27me3, this may create a positive feedback loop consistent with stable, long-term transcriptional repression of lineage commitment genes, whereas loci marked by H3K27me3 that do not recruit PRC1 are more sensitive to Suz12/PRC2 depletion and exhibit overall lower levels of this mark. In further support of a “protective” mechanism, we found that Bmi1 levels were markedly up-regulated on chromatin after Suz12 depletion, although the protein was not elevated in extracts, suggesting efficient sequestering (or redistribution) of Bmi1 on genes that must be silenced.

We note the parallels between our findings and studies in ES cells by Ku et al. (29), who surveyed the genome-wide overlap of bivalent promoters with Ring1B and PRC2 binding in ES cells. However, there are important differences between these two studies. First, these studies revealed the existence of two populations of bivalent genes based on Ring1B recruitment. Although we have not performed genome-wide studies on Bmi1, we have shown that very few genes are bivalent in myoblasts and myotubes, and of the genes that we have examined with detectable Bmi1 recruitment, none are bivalent. Second, Ku et al. (29) found that, in general, regulators of development were bound by PRC1. However, we have characterized in detail a notable exception to this classification, namely, *Myog*, which is not occupied by Bmi1 (Fig. 4*C*). Finally, the prior study found that depletion of Ring1B led to up-regulation of PRC1-positive bivalent promoters, in

striking contrast with our results, wherein loss of Bmi1 had no impact on expression of H3K27me3-marked, permanently silenced genes, indicating functionally different outcomes on bivalent and permanently repressed genes. Importantly, each of these findings reinforce the need for comparisons between pluripotent and committed cell types.

Given the opposing phenotypes of depleting PRC1 and PRC2 components in muscle, our observations diverge from a sequential (or synergistic) model for the action of these complexes. Interestingly, recent studies suggest that PRC1 and PRC2 may also play opposing roles in hematopoietic stem cell differentiation, wherein they appear to regulate distinct sets of genes (30). In addition, we note that, in contrast with Bmi1 or Ring1B suppression in muscle cells, which compromises differentiation, ES cells conditionally deleted for Ring1B exhibit defects in stem cell maintenance and are predisposed to differentiate (31). Furthermore, Suz12 depletion blocks ES cell differentiation while enhancing myogenic differentiation (our results and ref. 15). Both findings suggest major differences between these cell types.

Control of *Myog* Expression through H3K27me3. Our compendium of histone modifications points to a widespread role for H3K27me3, rather than H3K9me3, in myogenic differentiation. Consistent with this conclusion, Suz12 depletion markedly accelerated myogenic differentiation, complementing studies in which Ezh2 overexpression abolished differentiation (7). Our genome-wide dataset enabled us to discover a unique role for *Myog*, among the group of MRFs, as a target of this repressive methylation and imply that PRC2-mediated regulation of this gene suppresses its expression in myoblasts, and reversal of this mark is a pivotal force driving myogenic differentiation. Classical experiments demonstrated that enforced expression of MyoD1 can convert fibroblasts to skeletal muscle (32), and because *Myog* is a physiological target of MyoD1 which can, in turn, regulate MEF2c, it lies at a critical node that drives myogenesis (5, 6), making it an attractive candidate for control by an H3K27me3-mediated on-off switch. Indeed, our studies suggested the differentiation-dependent replacement of repressive modifications with activating marks on *Myog* regulatory regions, several of which exhibited hallmarks of enhancers (marked with p300, H3K4me1, PolII, and H3K27ac) and displayed myotube-specific enhancer activity. Suz12 depletion led to the loss of PRC2 and H3K27me3 on *Myog*, concomitant with premature and enhanced gene induction. Together, these studies suggest that this histone mark could represent part of a methylation-acetylation differentiation switch, helping to determine the timing of expression of this gene and thereby terminal differentiation. In addition, other mechanisms, such as active demethylation, are likely to play a role in removing the H3K27 methylation mark from this gene (9).

We note that in transgenic mouse studies, 133 bp of 5' flanking DNA was sufficient to confer correct spatiotemporal expression of *Myog* in embryos (33). However, the level of expression was considerably reduced (approximately 20%) as compared to constructs with additional flanking sequence, consistent with the contribution of other regulatory elements. Thus, our dataset represents a unique resource for discovery of regulatory elements, including promoters, enhancers, and noncoding RNAs.

A Genome-Wide Myogenic Landscape: Signatures of Developmental Plasticity? Our ChIP-seq data show that most developmental regulators are no longer bivalent, as they are in ES cells, yet genes encoding critical regulators of adipogenesis and osteogenesis, including the C/EBP family, PPAR- γ , and Runx2, exhibit features of active chromatin, in keeping with the fact that each is expressed in muscle (Figs. S6 and S8*B*). The epigenetic profiles for these genes stand in marked contrast to other lineage-determining transcription factors that are “locked” in a repressed state, and this could be the underlying basis for plasticity observed in skeletal muscle

cells. Whereas the presence of active marks could have been predicted on the basis of expression profiling, other features that we observed in our ChIP-seq compendium could not have been anticipated a priori. First, key regulators of osteogenesis and adipogenesis (*C/EBP β / δ* , *PPAR- γ* , and *Runx2*) were not bivalent and exhibited exclusively active marks, with the exception of *C/EBP α* , which exhibited a mixture of active and repressive marks. Second, whereas *Runx2* exhibited H3K4me2/3 and was devoid of H3K27me3, we note that the majority of genes thought to lie downstream of this master regulator, including a transcription factor (*Osterix*) essential for osteogenic differentiation, were not uniformly marked by active chromatin modifications, consistent with the need for a second, inductive event, such as exposure to bone morphogenetic proteins (BMPs). Third, inhibitors of myogenesis (*Twist*, *Fli1*, *PRDM16*) were heavily marked by H3K27me3 in myoblasts, and further, we have shown that both *Twist* and *PRDM16* recruit Bmi1, suggesting that they represent class II genes that must be potentially silenced in muscle (Fig. S9A).

Our results may also have significant implications for human diseases, such as obesity and atrophy, disorders characterized by an imbalance between adipose and muscle mass. These observations suggest the intriguing possibility that different mesodermal fates could be altered through modulation of distinct chromatin modifications. It may be possible to pharmacologically “push” chromatin modifications in one direction or the other, thereby redistributing the balance between the two types of tissue, although any such effort will have to consider the barriers that are imposed by distinct types of repressive chromatin, exemplified by our studies of H3K27 methylation and Polycomb recruitment.

- Berger SL (2007) The complex language of chromatin regulation during transcription. *Nature* 447:407–412.
- Li B, Carey M, Workman JL (2007) The role of chromatin during transcription. *Cell* 128:707–719.
- Bernstein BE, et al. (2006) A bivalent chromatin structure marks key developmental genes in embryonic stem cells. *Cell* 125:315–326.
- Mikkelsen TS, et al. (2007) Genome-wide maps of chromatin state in pluripotent and lineage-committed cells. *Nature* 448:553–560.
- Blais A, et al. (2005) An initial blueprint for myogenic differentiation. *Genes Dev* 19:553–569.
- Cao Y, et al. (2010) Genome-wide MyoD binding in skeletal muscle cells: A potential for broad cellular reprogramming. *Dev Cell* 18:662–674.
- Caretti G, Di Padova M, Micales B, Lyons GE, Sartorelli V (2004) The Polycomb Ezh2 methyltransferase regulates muscle gene expression and skeletal muscle differentiation. *Genes Dev* 18:2627–2638.
- Blais A, van Oevelen C, Margueron R, Acosta-Alvear D, Dynlacht BD (2007) Retinoblastoma tumor suppressor protein-dependent methylation of histone H3 lysine 27 is associated with irreversible cell cycle exit. *J Cell Biol* 179:1399–1412.
- Seenundun S, et al. (2010) UTX mediates demethylation of H3K27me3 at muscle-specific genes during myogenesis. *EMBO J* 29:1401–1411.
- Pajcini KV, Corbel SY, Sage J, Pomerantz JH, Blau HM (2010) Transient inactivation of Rb and ARF yields regenerative cells from postmitotic mammalian muscle. *Cell Stem Cell* 7:198–213.
- Duncan EM, et al. (2008) Cathepsin L proteolytically processes histone H3 during mouse embryonic stem cell differentiation. *Cell* 135:284–294.
- Liu Y, Chu A, Chakroun I, Islam U, Blais A (2010) Cooperation between myogenic regulatory factors and SIX family transcription factors is important for myoblast differentiation. *Nucleic Acids Res* 38:6857–6871.
- van Oevelen C, et al. (2010) The mammalian Sin3 proteins are required for muscle development and sarcomere specification. *Mol Cell Biol* 30:5686–5697.
- Stock JK, et al. (2007) Ring1-mediated ubiquitination of H2A restrains poised RNA polymerase II at bivalent genes in mouse ES cells. *Nat Cell Biol* 9:1428–1435.
- Pasini D, Bracken AP, Hansen JB, Capillo M, Helin K (2007) The polycomb group protein Suz12 is required for embryonic stem cell differentiation. *Mol Cell Biol* 27:3769–3779.
- Ait-Si-Ali S, et al. (2004) A Suv39h-dependent mechanism for silencing S-phase genes in differentiating but not in cycling cells. *EMBO J* 23:605–615.
- Pauler FM, et al. (2009) H3K27me3 forms BLOCs over silent genes and intergenic regions and specifies a histone banding pattern on a mouse autosomal chromosome. *Genome Res* 19:221–233.
- Hu E, Tontonoz P, Spiegelman BM (1995) Transdifferentiation of myoblasts by the adipogenic transcription factors PPAR gamma and C/EBP alpha. *Proc Natl Acad Sci USA* 92:9856–9860.
- Lee KS, et al. (2000) Runx2 is a common target of transforming growth factor beta1 and bone morphogenetic protein 2, and cooperation between Runx2 and Smad5 induces osteoblast-specific gene expression in the pluripotent mesenchymal precursor cell line C2C12. *Mol Cell Biol* 20:8783–8792.
- Heintzman ND, et al. (2009) Histone modifications at human enhancers reflect global cell-type-specific gene expression. *Nature* 459:108–112.
- Visel A, et al. (2009) ChIP-seq accurately predicts tissue-specific activity of enhancers. *Nature* 457:854–858.
- Kim TK, et al. (2010) Widespread transcription at neuronal activity-regulated enhancers. *Nature* 465:182–187.
- Frith MC, et al. (2004) Detection of functional DNA motifs via statistical overrepresentation. *Nucleic Acids Res* 32:1372–1381.
- Postigo AA, Dean DC (1999) Independent repressor domains in ZEB regulate muscle and T-cell differentiation. *Mol Cell Biol* 19:7961–7971.
- Schoeftner S, et al. (2006) Recruitment of PRC1 function at the initiation of X inactivation independent of PRC2 and silencing. *EMBO J* 25:3110–3122.
- Simon JA, Kingston RE (2009) Mechanisms of polycomb gene silencing: knowns and unknowns. *Nat Rev Mol Cell Biol* 10:697–708.
- Eskeland R, et al. (2010) Ring1B compacts chromatin structure and represses gene expression independent of histone ubiquitination. *Mol Cell* 38:452–464.
- Rosen GD, et al. (1992) Roles for the integrin VLA-4 and its counter receptor VCAM-1 in myogenesis. *Cell* 69:1107–1119.
- Ku M, et al. (2008) Genomewide analysis of PRC1 and PRC2 occupancy identifies two classes of bivalent domains. *PLoS Genet* 4:e1000242.
- Majewski IJ, et al. (2010) Opposing roles of polycomb repressive complexes in hematopoietic stem and progenitor cells. *Blood* 116:731–739.
- Leeb M, Wutz A (2007) Ring1B is crucial for the regulation of developmental control genes and PRC1 proteins but not X inactivation in embryonic cells. *J Cell Biol* 178:219–229.
- Tapscott SJ, et al. (1988) MyoD1: A nuclear phosphoprotein requiring a Myc homology region to convert fibroblasts to myoblasts. *Science* 242:405–411.
- Yee SP, Rigby PW (1993) The regulation of myogenin gene expression during the embryonic development of the mouse. *Genes Dev* 7:1277–1289.

Materials and Methods

Preparation of Chromatin and ChIP. ChIP was performed as described (8), and sonication was performed to obtain chromatin fragments of approximately 250 bp whereas MNase digestion produced approximately 150 bp fragments. Antibodies used for ChIP are listed in *SI Materials and Methods*. Quantitative ChIP for validation was performed using three or more independent biological replicates, except as noted. ChIP enriched DNA was analyzed using real-time PCR (qChIP), and in every case, background was assessed using a negative control antibody (rabbit IgG). For all experiments shown, the IgG control produced an average enrichment $\leq 0.05\%$ of the input for a given site.

ChIP-Seq. For ChIP-seq, titrations of chromatin and antibodies were performed to ensure linear results in all ChIP reactions. Libraries for Illumina GA sequencing, data processing, and filtering procedures are described in *SI Materials and Methods*.

Quantitative RT-PCR (RT-qPCR) and RNAi Experiments. All procedures are described in *SI Materials and Methods*.

Immunofluorescence. Immunofluorescent detection of MHC was performed as described (8).

Enhancer Assays. All procedures are described in *SI Materials and Methods*.

ACKNOWLEDGMENTS. We thank D. Reinberg, R. Kingston, L. Dailey, and K. Helin for reagents. We thank C. van Oevelen for early contributions to ChIP-seq development. We thank the New York University Cancer Institute Genomics facility for their services and Z. Tang and S. Brown for assistance with analysis of ChIP-seq data. B.D. was supported by National Institutes of Health Grants CA077245, GM067132-07, and GM067132-07S1. V.V. received support from a T32/NIH-NCI training grant and is currently supported by an American Cancer Society postdoctoral fellowship. M.M. was supported by National Science Foundation Integrative Graduate Education and Research Traineeship (IGERT) Grant 0333389.